C2FUEL - This project has received funding from the European Union's Horizon 2020 research and innovation programme under grant agreement No 838014
The C2FUEL project results presented reflect only the author's view. The Commission is not responsible for any use that may be made of the information it contains.

C2FUEL

Carbon Captured Fuel and Energy Carriers for an Intensified Steel Off-Gases based Electricity Generation in a Smarter Industrial Ecosystem

Deliverable

D4.2 – Catalysts synthesized for FA production

WP4 – Development and up-scale of FA production

Project information

Grant Agreement n°	838014
Dates	1st June 2019 – 31st May 2023

PROPRIETARY RIGHTS STATEMENT

This document contains information, which is proprietary to the C2FUEL Consortium. Neither this document nor the information contained herein shall be used, duplicated or communicated by any means to any third party, in whole or in parts, except with prior written consent of the C2FUEL consortium.

Document Status

Document information

Deliverable name	Catalyst synthesized for FA production
Responsible beneficiary	Eindhoven Technical University
Contributing beneficiaries	Eindhoven Technical University
Contractual delivery date	M18 – 30/11/2020
Actual delivery date	M26 – 05/07/2021
Dissemination level	Confidential

Document approval

Name	Position in project	Organisation	Date	Visa
C. MAKHLOUFI	Coordinator	ENGIE	05/02/2021	OK
L.NAIGLIN	Project Management Officer	AYMING	05/02/2021	OK
P. OLIVIER	Project Management Officer	ENGIE	05/02/2021	OK
M. C. Figueiredo	WP LEADER	TU/e	03/02/2021	OK

Document history

Version	Date	Modifications	Authors
V1	15/01/2021	1ST DRAFT	Tim Wissink, Marta Costa Figueiredo/ TUE
V2	22/01/2021	2nd DRAFT	Tim Wissink, Marta Costa Figueiredo/TUE
V3	27/01/2021	Minor modifications	P.OLIVIER/ENGIE
V4	03/02/2021	Minor modifications	Tim Wissink, Marta Costa Figueiredo/TUE
V5	05/02/2021	Minor modifications	P.OLIVIER/ENGIE
VF	05/02/2021	Final check	L. NAIGLIN/AYMING
VF	05/07/2021	Final release for confidentiality reasons	L. NAIGLIN/AYMING

Table of Contents

List of Figures

List of Tables

Deliverable report

1 Executive Summary

1.1 Description of the deliverable content and purpose

In search for new sources for products and energy storage, attempts are made to use the waste product CO_2 as a source for valuable chemicals[1]. Formic acid is one such molecule that is widely used as feedstock in chemical industry[2] and is promising as a hydrogen carrier for energy storage, dispatch and on demand production.[3] Formic acid can be produced using renewable energy and CO_2 from air. WP4 aims to develop a lab-scale formic acid production demonstrator that will produce sustainable formic acid by using H_2 (from SOFC) or H_2O, electrons and CO_2. Within this WP, the development of catalysts able to (electro) catalytically convert CO_2 to formic acid is expected. The choice of the most suitable catalysts is based on an initial literature study, a screening of several catalysts to find the most active ones and subsequently an in-depth research on the chosen catalyst to improve its activity and lifetime. This deliverable describes the initial literature study and the screening of catalysts that are most active in CO_2 reduction to formic acid. Based on this deliverable, a consolidate choice can be made on which selection of catalysts should be investigated further to obtain a stable, active and economically viable catalyst for industrial-scale formic acid production processes from CO_2.

1.2 Brief description of the state of the art and the innovation breakthroughs

1.2.1 Hydrogenation catalysts

Heterogeneous catalysis has known practical advantages for continuous operation and product separation, therefore the number of catalysts reported in literature is increasing. Though the number of heterogeneous catalysts for CO_2 hydrogenation to formic acid reported is yet relatively limited. Alvarez *et al.* summarized catalysts reported up to 2017 in their review.[1] The most popular active metals studied are Pd, Au and Ru on supports such as activated carbon, alumina and titania. Pd and Au are the most used catalysts, with the catalytic performance showing a strong dependency on the support material. Here, the most promising supports were found to be dependent on the active metal, with Pd preferring hydrophobic carbon-based supports, while Au should be combined with a hydrophilic support such as Al_2O_3 and TiO_2.[1]

Even though the state-of-the-art catalysts seem sufficiently active and selective,[1,4,5] the equilibrium concentrations reached remain low due to the reaction being thermodynamically unfavorable.[4] One of the commonly employed strategies is to reduce formic acid within the reaction mixture through the formation of adducts/complexes.[4] Often, nitrogenous bases or alkali is used for this purpose.[4,5] Promising results have been obtained using tertiary amines.[6,7] In several cases, bicarbonates were used as reactant instead of CO_2 which was often reported to be more active and involved in the reaction mechanism of CO_2 reduction. When using gaseous CO_2 as reactant, concentrations reported are generally (far) below one molar formic acid.

Even though there are examples of unsupported metal catalysts and heterogenized molecular catalysts in CO_2 hydrogenation, we will focus on supported metal catalysts with supported commercial Au nanoparticles being the most promising candidate. Support materials increase the number of active sites by finely dispersing the active metal on the nanometer scale. Secondly, supports increase the stability of the catalyst by inhibition of sintering of the active metal. Also the support can show interactions that alter the electronic structure of the catalyst and enhance its activity.[1]

To circumvent separation of a molecular complex catalyst in homogeneous formic acid production, Preti *et al.*[8,6,9] developed and patented in cooperation with BASF[10] a heterogeneous catalyst to produce HCOOH/NEt_3 adducts. One of their works[6] has employed a commercially available heterogenous catalyst: titania-supported gold (1 wt% Au/TiO_2, AURO*lite* from Mintek). To the best of our knowledge, this is the most stable heterogeneous catalyst reported to date, a TON of 18040 was achieved, corresponding to a TOF of about 20 h^{-1}. Gas analysis revealed the formation of 63 mmol CO accumulated in 37 days, with no other organic products being detected within the extracted products, thereby showing the very high selectivity of the employed catalyst. The selectivity was not affected by CO formation, presumably from gold catalyzed reverse water gas shift reaction. The conversion of neat amine into adducts is complete under CO_2/H_2 1:1 pressure above 41 bar and at 40°C. A stability test was conducted between 130 bar and 180 bar H_2/CO_2 over 37 days showing no deactivation of the catalyst. Reproductions including CO impurity effects showed similar activities and stability.[9] This catalyst was further studied by Filonenko *et al.*[7] Several supports were screened and in their reaction conditions, Al_2O_3 was found to be two times more active than the TiO_2 support. This was explained by active involvement of the basic sites of Al_2O_3 with the Au nanoparticles.[7]

NEt_3 has been used in most publications as the base for the CO_2 hydrogenation, however, the formed salt does not allow for direct thermal splitting.[6,11] Care should be taken during the separation as the employment of temperatures above 150 °C result in the decomposition of formic acid. Low-boiling amines such as NEt_3 result in stable azeotropes, rendering separation through (vacuum) distillation impossible.[6] To obtain virtually pure formic acid, the authors employed a amine-exchange method found within the patent literature: the low-boiling amine is replaced by a high-boiling amine such as imidazoles or tri-n-hexylamine.[6] The obtained salt can then be decomposed in formic acid and the high-boiling base through distillation, but the base exchange leads to an undesired additional step in the proposed process, similar to the steps proposed in literature with homogenous catalysts.[11]

In an attempt to circumvent the additional separation step, Schaub *et al.*[11] reported the usage of other trialkylamines to form salts that are immiscible with free amine. One of bases reported is $NHex_3$ (trihexylamine), which allowed for thermal cleavage under mild conditions (150 °C, 150 mbar). The disadvantage of this approach is that the usage of this base as the only reactant/solvent does not result in observable reaction despite the usage of a catalyst known to show high formic acid activity. Calorimetry revealed that the reaction is not feasible in pure $NHex_3$ due to the amine protonation not supplying sufficient reaction enthalpy. To resolve this, the authors

employed polar hydrogen-bonding solvents such as diols. Here, it was hypothesized the addition of solvents containing an OH-group stabilized the formate anion through the formation of hydrogen bonds.[11] As the addition of more solvents could lead to more complex and expensive separation steps, an interesting research topic could be the usage of ethoxylated/propoxylated tertiary amines.

1.2.2 Electrocatalytic CO_2 reduction to formic acid

Electrochemical CO_2 reduction allows for direct utilization of renewable energy. A potential applied to catalytically active electrodes, immersed in CO_2 saturated electrolyte or humidified CO_2 gas, results in selective reduction of CO_2 to formate.[12] The main other advantages are operation at ambient pressure and temperature. Electrochemical formic acid (FA) production seems to give a trade off between high faradaic efficiency (FE) and high current density (CD) (OPEX and CAPEX, respectively). Selectivity depends on pressure, potential and current density, pH, electrolyte type and concentration, electrode(catalyst) material and morphology and aqueous or non-aqueous solvent.[13] A balance needs to be found where the supply of electrons, protons and CO_2 to the catalyst surface perfectly matches in order to have high FE towards FA. Thereby avoiding production of H_2 (deficiency of CO_2) or low current densities (deficiency of electrons and CO_2). This can be done by optimizing catalysts, charge transfer, CO_2 diffusion and pH.[13]

The past decades increased efforts in electrochemical reduction of CO_2 have led to significant advances[14,15,16]. The most promising catalytic active and selective metals are Tin (Sn), indium (In), bismuth (Bi), cobalt (Co) and lead (Pb).[17] These materials and the combinations thereof achieve relatively high efficiencies in existing literature (around 90%). Of these metals the use of Pb is least attractive due to its poisonous properties.

The electrocatalytic reduction of CO_2 to formate can be performed at high faradaic efficiency but is limited by current density for industrial application. In this work, gas diffusion electrodes (GDE) are studied to optimize the three-phase boundary dynamics, where gaseous CO_2 and liquid water are reduced at the solid catalyst surface to formate, overcoming CO_2 diffusion limitations through the electrolyte.[18] Indium and Bismuth are chosen as catalysts as they have proven to give high faradaic efficiencies.[19] We used flame spray pyrolysis (FSP) for the synthesis of the catalyst. With FSP, well defined small nanoparticles of In_2O_3 and Bi_2O_3 can be synthesised and doped with other metal(-oxides), to search for a more stable and highly active electrocatalyst in CO_2 to formate conversion. The In_2O_3 nanoparticles are doped with Cu, Pd, Co, CeO_2 and ZrO_2 and the activity in CO_2 reduction to formate are compared. Industrially relevant faradaic efficiencies above 90% and current densities up to 300 mA/cm^2 are achieved.

1.3 Corrective action (if relevant)

- Due to COVID19 pandemic, the lab work was delayed by two months and so the deliverable.
- In M18, a new PhD candidate was hired at the TU/e, for the development of the heterogeneous hydrogenation path. Experimental results will be shown in the next deliverables.

1.4 IPR issues (if relevant)

Not applicable

2 Transition metal doped indium and bismuth catalyst for electrochemical CO_2 reduction to formic acid

2.1 Introduction

The electrocatalytic reduction of CO_2 to formate is the first two electron reduction product of CO_2 besides CO. In an electrochemical cell a cathode and anode are used to reduce CO_2 at the cathode and oxidize water (or any other molecule of interest) at the anode. Combined reactions give the overall reaction as shown below:

$$1.\ CO_2 + 2H^+ + 2e^- \rightarrow CHOOH$$

$$2.\ H_2O \rightarrow \frac{1}{2}O_2 + 2e^- + 2H^+$$

$$CO_2 + H_2O \rightarrow CHOOH + \frac{1}{2}O_2$$

As can be seen from reaction 1, at the cathode, CO_2, protons and electrons need to be combined, coming from three different phases, gaseous, liquid and solid cathode respectively. As the CO_2 molecule is a thermodynamically very stable molecule with a high kinetic activation barrier, a highly active catalyst is essential to obtain fast kinetics. A catalyst that lowers the kinetic energy barrier for this reaction results in a lower needed overpotential. A lower potential result in less energy consumption, essential for industrial application. This (conductive) catalyst is used as cathode and needs to be configurated such that enough CO_2, electrons and protons reach the catalyst surface. At the same time the catalyst needs to be selective for CO_2 reduction over water reduction, to achieve high faradaic efficiency. The reaction can already be performed at high faradaic efficiency but is limited by current density for industrial application. Also, the catalyst needs to be stable over long time to reduce the need for frequent replacement.

2.2 Catalyst synthesis

The catalysts were synthesized by flame spray pyrolysis. FSP is a well-established technique which is commercially applied to make catalyst particles.[20] In short, a metal nitrate precursor solution containing, for example In, and possibly a dopant metal such as Co, Cu or Pd enters an FSP setup together with a gas flow containing oxygen and methane. This mixture is ignited to make a flame in which the metal nitrates form droplets and combust and subsequently nucleate and condensate into metal(oxide) particles.

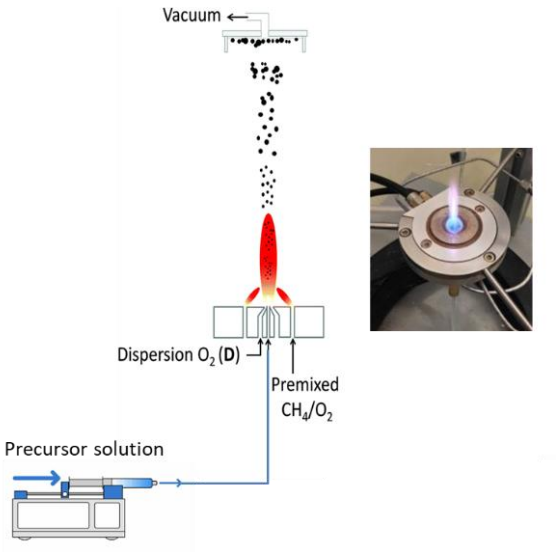

Figure 1: Flame Spray Pyrolysis (FSP) setup

The catalysts synthesized are listed in Table 1: . These dopants were chosen because Co has shown to greatly improve the electrochemical CO_2 to formate conversion efficiency in nanosheet configurations.[21] To see the effect of Co doping on formate efficiency formation, a 5 wt% Co doping is used. Also Pd has shown to exhibit very low overpotential for formate formation,[22] but when larger potentials are applied, hydrogen evolution dominates.[23,24] In an attempt to achieve low overpotential for formate formation while maintaining the high efficiency at large current densities, In_2O_3 is doped with 5 wt% Pd. As Cu is a well-known catalyst for CO_2 electroreduction, the In_2O_3 nanoparticles are also doped with Cu. CeO_2 is interesting for its easily reducible nature. It is used as a support for oxygen exchange and storage.[25] For CO_2 to formate reduction catalyst the surface composition is under debate. It is shown that the metal-oxide phase could persist under reducing conditions and might be crucial to maintain high activity for CO_2 reduction.[26] An oxygen exchange material such as CeO_2 could be of interest to provide in support interaction via e.g. oxygen exchange or CO_2 adsorption on a CeO_x site. Nanoparticles synthesized by FSP using a 10:1 In_2O_3:CeO_2 ratio are used. For the same reason ZrO_2 is also tried.

Table 1: List of catalysts synthesized by FSP

Catalyst	Composition
In_2O_3	5 nm
ZrO_2-In_2O_3	10 wt%
CeO_2-In_2O_3	10 wt%
Co-In_2O_3	5 wt%
Pd-In_2O_3	5 wt%
Cu-In_2O_3	5 wt%
Ni-In_2O_3	5 wt%
Bi_2O_3	10-20 nm
In-Bi-oxide	10-20 nm

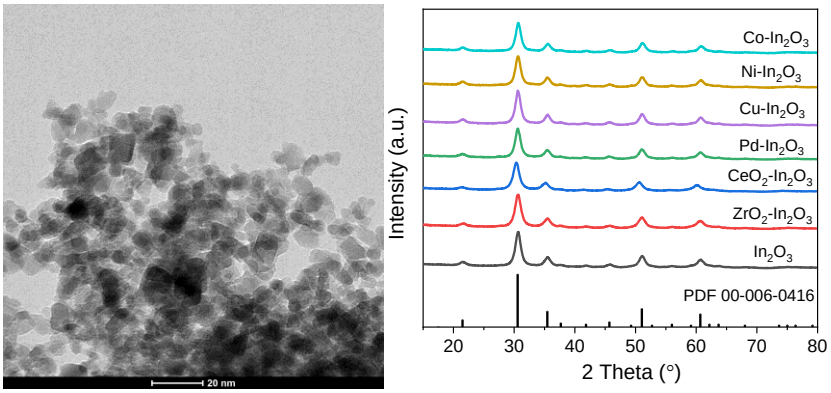

Figure 2: a) TEM image of In2O3 nanoparticles, b) XRD of (doped) In2O3 nanoparticles.

The size of the particles is around 5 nm as observed in the TEM image in Figure 2. Catalyst particles below 10 nm contain a high degree of undercoordinated surface atoms, which have proven to be more active in catalytic reactions.[27] The precise effect of different particle sizes below 10 nm on the efficiency and overpotential for CO_2 reduction to formic acid is yet unknown, and needs to be studied. From the XRD spectra we learn that the morphology and size distribution are unchanged for the doped In_2O_3 nanoparticles. No phases can be observed from the dopant atoms in the XRD spectra, which indicates the very small cluster sizes or possibly single atom nature of the dopants. More refined analysis techniques such as STEM-EDX are needed to identify the morphology and position of the dopant atoms.

These catalysts were dispersed in an ink with a binder and high surface area, conductive carbon particles and deposited in a GDE (**Erreur ! Source du renvoi introuvable.**) and studied in an electrochemical flow cell as illustrated inFigure 3.

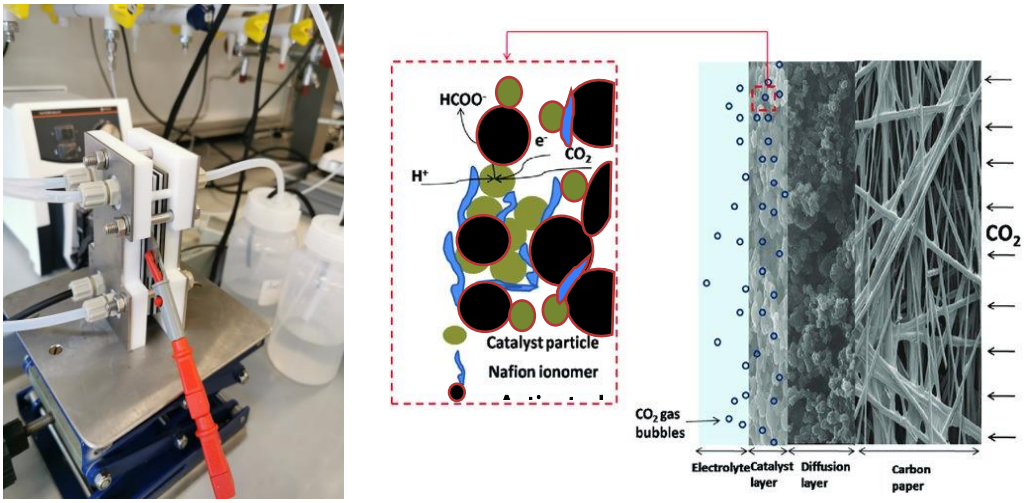

Figure 3: Electrochemical flow cell and Gas Diffusion Electrode setup.

In an electrochemical flow cell, two compartments are separated by an ion exchange membrane. In the cathode compartment, a liquid electrolyte is pumped along the GDE as illustrated above. CO_2 flows from the backside of the GDE through the finely dispersed carbon particles and catalyst particles. The GDE is connected to a power source to apply a certain potential, delivering the necessary electrons to the catalyst on the GDE. On the anode compartment, water from the flowing liquid electrolyte is oxidized by a platinum mesh to oxygen. The protons selectively travel through the ion exchange membrane to the cathode compartment, where they are reduced with CO_2 to formic acid. For industrial applications, the compartments can be stacked to make larger cells and achieve higher productivity.

Table 2: List of prepared GDE sheets.

GDE	Metal np loading (mg/cm²)
1) In_2O_3	0.17
2) In_2O_3	0.22
3) Co-In_2O_3	0.17
4) CeO_2-In2O3	0.09
5) Pd-In_2O_3	0.49
6) ZrO_2-In_2O_3	0.19
7) Cu-In_2O_3	0.12

2.3 Experimental Results

2.3.1 Preliminary GDE characterization

The GDE configuration has a critical influence on the reaction conditions at the catalyst surface. The provision of CO_2, water and electrons at roughly equal ratios to the catalyst surface depends on the porosity and hydrophobicity of the GDE. This is in part controlled by the relative concentration of catalyst, carbon particles and Nafion binder in the catalyst layer.

Therefore, a study on the effect of carbon content in the catalyst ink was performed. Carbon is added to the catalyst to increase surface dispersion and avoid particle sintering. However, carbon will increase the thickness of the catalyst layer, which might negatively affect the reaction performance. The results in Table 3Table 3: Effects of catalyst composition in the GDE on the CO_2 reduction activity show that changing the carbon content from 40 wt% to 20 wt% does not have a large impact on the activity of the catalyst, but removing the carbon totally does have a detrimental effect on the faradaic efficiency and needs overpotential to reach a current density of 200 mA/cm^2. This indicates that the dispersion of catalyst particles over a carbon particles framework leads to a better diffusion of CO_2 to the catalyst surface and possibly a better conductivity of electrons to the catalyst particles.

Table 3: Effects of catalyst composition in the GDE on the CO_2 reduction activity.

Catalyst composition	Metal NP's	Activated Carbon	Nafion binder	Max FE with In2O3 at -200 mA/cm2	Average Potential needed for -200 mA/cm2
Ratio 1	39 wt%	39 wt%	22 wt%	93.5 %	3.0 V vs RHE
Ratio 2	59 wt%	20 wt%	21 wt%	89.2 %	3.1 V vs RHE
Ratio 3	79 wt%	0 wt%	21 wt%	55.4 %	3.7 V vs RHE

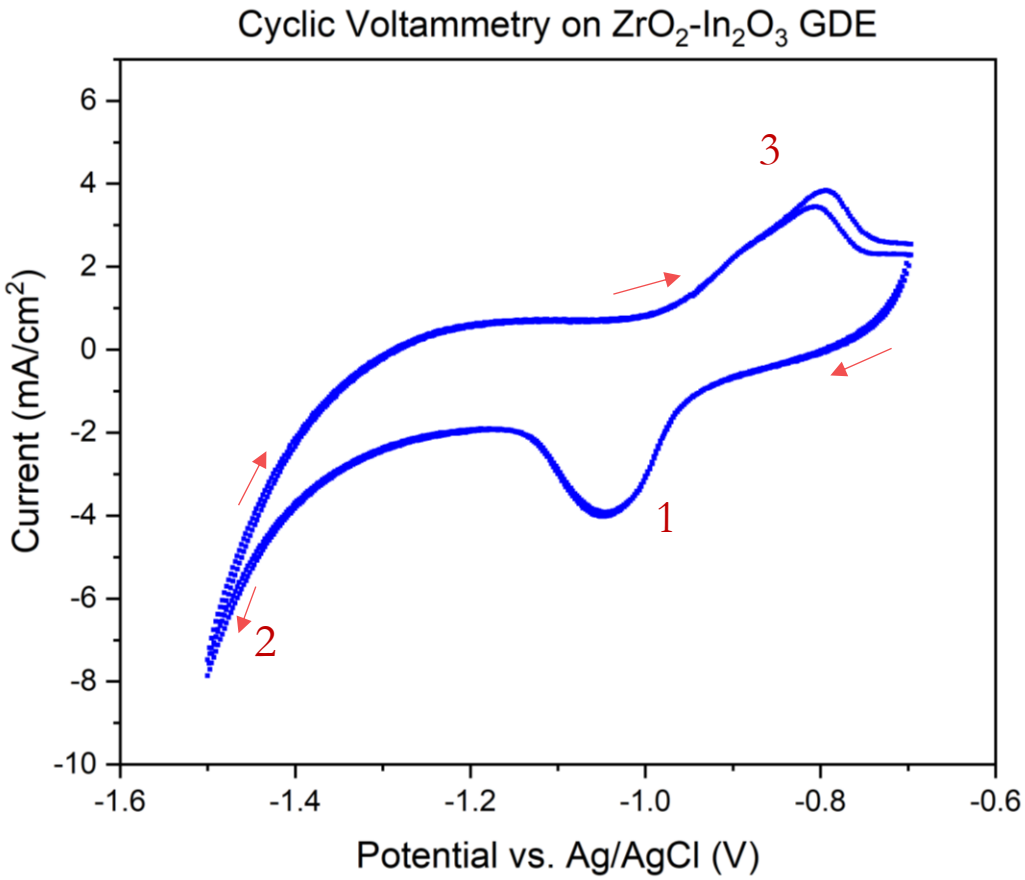

Figure 4: Cyclic Voltammetry on ZrO2-In2O3 catalyst.

Cyclic voltammetry (CV) was performed to confirm the presence of the metal on the electrode, by identifying its redox features. The resulting graph in Figure 4 suggests that the reduction of the catalyst nanoparticles happens in the first reduction cycle. After the first reduction cycle, the next cycles do not show any significant change in reduction currents of oxides to metallic nanoparticles. The features numbered in Figure 2 correspond to 1: metal-oxide reduction to metallic or mixed oxidation states of the catalyst, 2: reduction of H_2O and CO_2, which cannot be distinguished based on cyclic voltammetry and 3: oxidation of (mixed) metal catalyst back to the metal-oxides. For reduction of CO_2, the applied potential should be more negative than -1.4 V vs Ag/AgCl. Extended tests by XPS and RAMAN will be used to confirm the reduced state of the catalysts during CO_2 reduction.

2.3.2 Characterization of Indium based catalysts

For industrially relevant applications, the current density needs to be higher than 100 mA/cm^2.[28,29] Also, current instead of potential will be applied to the catalyst, as applying current controls the electrons reaching the catalyst surface and thus the kinetics of the reaction. Chrono Potentiometry (CP) is applied in the search for suitable electrocatalysts, at industrial relevant conditions. GDE's were made, aiming for a catalyst nanoparticle loading of 0.2 g/cm^2. Current densities from 50 mA/cm^2 up to 300 mA/cm^2 were applied for 1 hour with steps of 50 mA/cm^2. For every experiment, a GDE was cut from the sheet that was large enough for all experiments in one series, to

ensure the same GDE characteristics. The pH of the CO_2 saturated electrolyte was measured to be stable around 7.4 before and after every experiment. Concentrations were analysed by HPLC. Faradaic efficiencies are calculated by dividing the number of electrons that went to formic acid over the total amount of electrons put into the cell, according to equation 1:

$$\text{Equation 1:} \quad FE = \frac{[FA]*V*n}{I*t}$$

with '[FA]' the concentration of formate in the cathode compartment, 'V' the electrolyte volume, 'n' the consumed electrons per formate molecule, 'I' the current density and 't' the time. The series are repeated for several doped In_2O_3 nanoparticles. The resulting activities are compared to the In_2O_3 without doping as shown in Figure 5 and Figure 6.

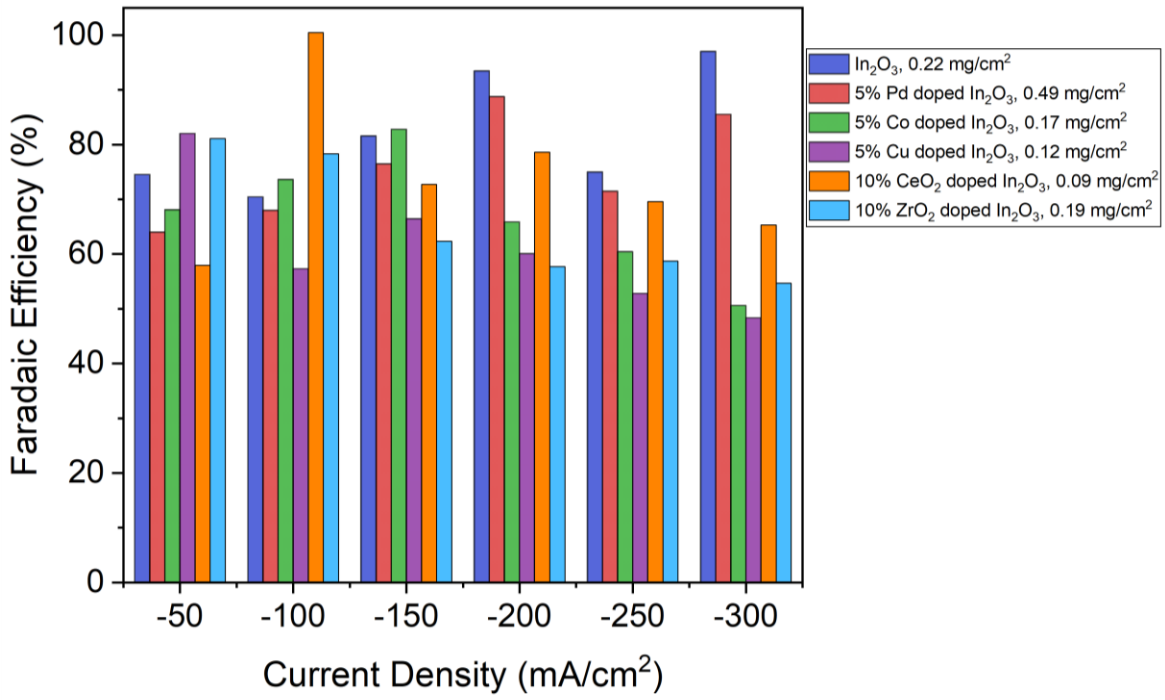

Figure 5: Effect of doping In2O3 with transition metals on the FE towards formate after one-hour chrono potentiometry at ambient temperature and atmospheric pressure.

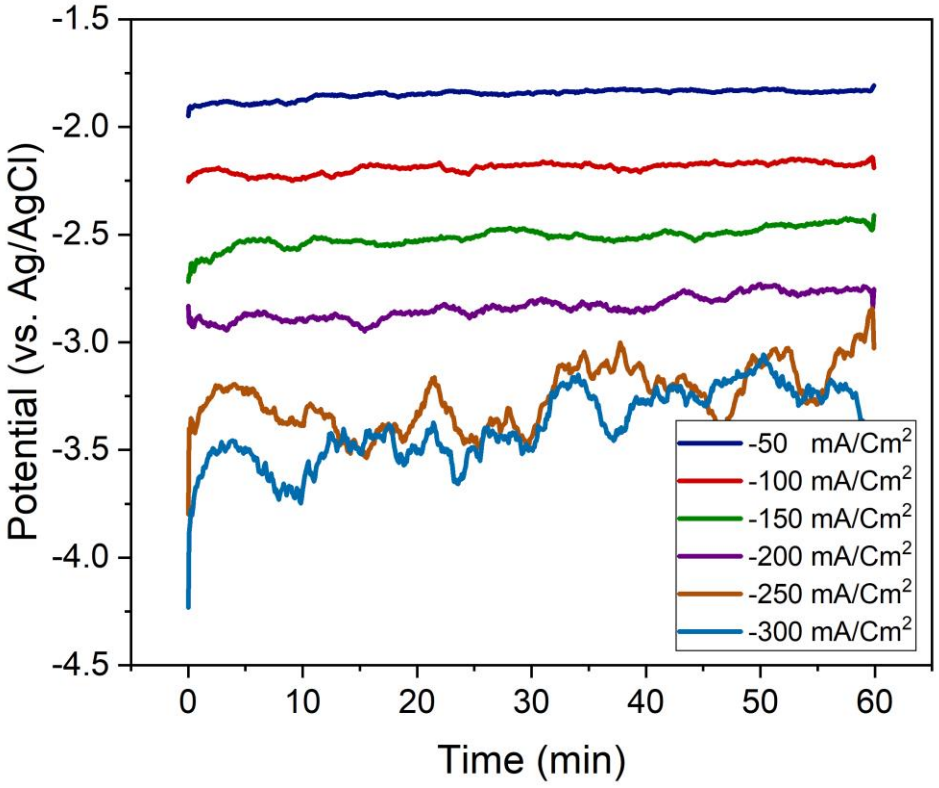

Figure 6: Recorded potentials needed for 1h chrono potentiometry between 50 and 300 mA/cm² on Pd-doped In_2O_3 at ambient temperature and pressure.

The first FE measured on the non-doped In_2O_3 samples show that the FE is approaching close to a 100% with increasing current density to 300 mA/cm². It is thereby the most active and selective catalyst of this series of experiments. The dopants do not seem to increase the faradaic efficiency towards formate for one-hour CO_2 reduction. The trend of decreasing efficiency after -150 mA/cm² could be a result of limitations by CO_2 diffusion. Low catalyst loading could also cause the decrease in FE towards higher current densities due to limited availability of catalyst surface area. It results in larger applied potential to achieve the same high current density, which in turn leads to more hydrogen evolution and thus lower FE. As long as the lowest loading that is used in this series is not limiting for the used current densities, the different catalysts can be compared. We do not observe a trend between catalyst loading and FE at high current density from this data, so we assume that the catalyst loading is sufficient to compare catalysts with respect to each other. No other liquid CO_2 reduction products were observed by NMR and HPLC by any of these catalysts, leading to the conclusion that only formate and gasses like CO, H_2 and possibly other small hydrocarbons were formed. The potentials needed to apply 50 to 300 mA/cm² are shown in Figure 6 for Pd-doped In_2O_3. This catalyst exhibited the lowest needed potentials for CO_2 reduction to formate, though the other catalysts show similar trends and potentials deviate only slightly from the Pd doped In_2O_3. The Co doped In_2O_3 required the largest potential up to roughly 4.0 V for 300 mA/cm². The large variation

in potential at larger current densities is because of hydrogen bubble formation that disturbs the conductivity of the GDE-electrolyte interface.

Overall, the Cu and ZrO_2 doped samples show the lowest efficiency towards formate. This could be explained by the affinity for the Cu-carbon bond,[30,15] leading to the formation of CO and possibly further reduction products of CO. Feaster *et al.*[15] showed that the formation of formate happens via the binding of oxygen atoms to the surface instead of carbon, explaining a decreased efficiency to formate for Cu. The ZrO_2 doped In_2O_3 shows a lower efficiency than for CeO_2, this might be a consequence of ZrO_2 relative stability and is therefore less active in the catalytic reaction and possible oxygen exchange. The Co doped samples show a decreased FE efficiency compared to pure In_2O_3, reaching max 83% at 150 mA/cm^2. This suggests that in this configuration, Co tends to form CO instead of formate. Although the CeO_2 doped sample shows an efficiency of 100.5% at 100 mA/cm^2, this efficiency looks like an outlier in the trend. After 30 minutes in this same experiment an efficiency of only 69.6% was measured, which was in line with the observed trend from the other current densities. Discarding this measurement would make the CeO_2 less selective, but we do note that for a very low catalyst loading (0.09 mg/cm^2), the efficiencies are relatively high at larger current densities compared to the other catalysts in this series. It would be interesting to study this catalyst at larger loadings. The Pd doped In_2O_3 reached a relatively high FE of 88.8% at -200 mA/cm^2 and has a larger efficiency than most other catalysts for the higher current densities.

SEM analysis without EDX do not provide much insight on the catalyst morphology as the nanoparticles are too small to be observed by SEM at this resolution (Figure 7). SEM images show the activated carbon covered GDE, the significantly smaller catalyst particles could be the small dots observed on the carbon particles, but without EDX, no conclusive information can be given. TEM measurements are necessary to see (changes in) the catalyst morphology and dispersion. However, SEM shows that all the catalysts have similar morphologies on the GDE surface.

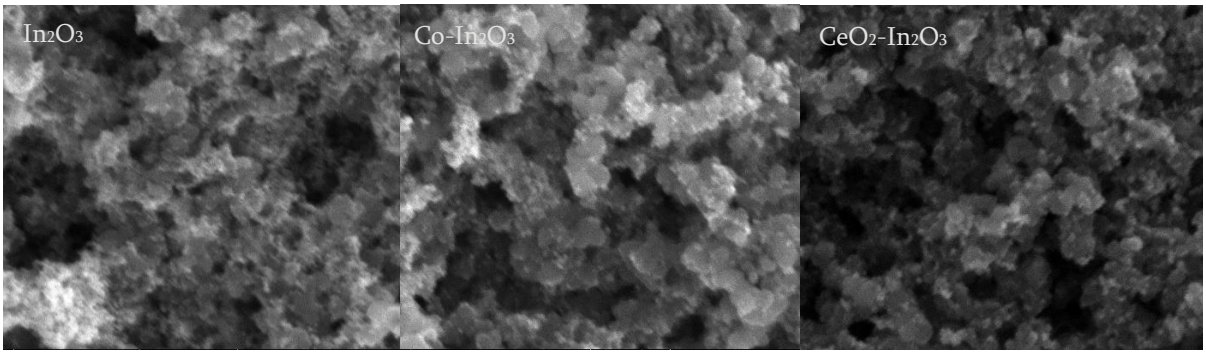

Figure 7: SEM images of GDE covered by activated carbon with In2O3, Co-In2O3 and CeO2-In2O3 nanoparticles.

2.3.3 Characterization of Bismuth based catalysts

Not only In_2O_3 has shown to give high faradaic efficiencies towards formate, also Bismuth has been reported to give very high efficiencies for large current densities.[31] Therefore, Bi_2O_3 particles as well as Bi-In-oxide were also synthesized by FSP and deposited into a GDE. SEM-EDX show that the Bi_2O_3 is well dispersed over the catalyst surface. TEM images show that the particles are slightly larger than the Indium particles with sizes up to 20 nm. XPS and XRD show a phase pure Bi_2O_3 catalyst with predominantly the tetragonal β-Bi_2O_3 phase, corresponding to the surface lattice orientation (201) as observed in XRD.

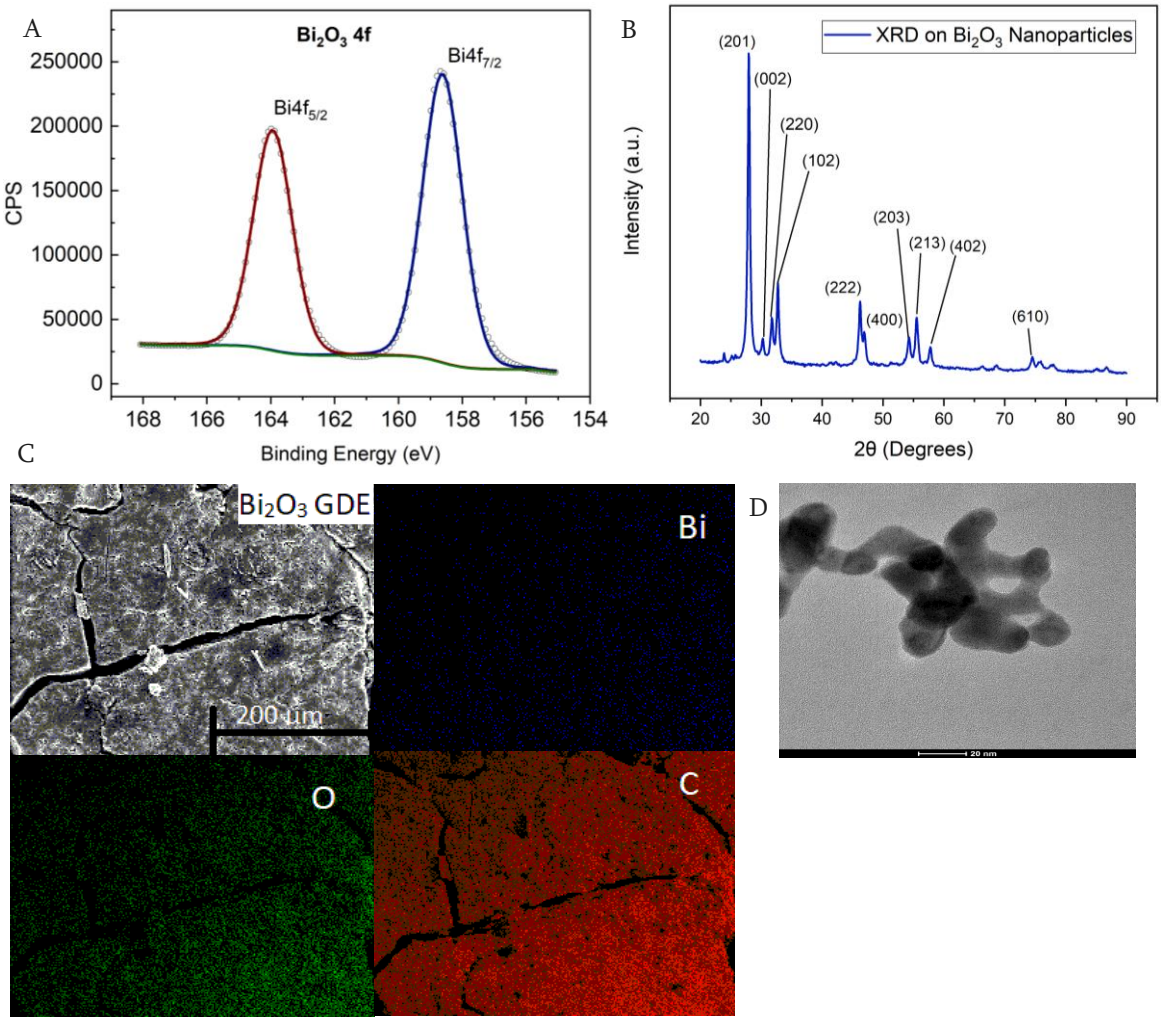

Figure 8: Catalyst and GDE characterization of Bi2O3 nanoparticles made by FSP. a) TEM image, b) XPS spectrum of the Bi4f region showing the Bi(III) oxidation state, c) XRD of Bi2O3, showing predominantly the (201) crystal orientation, d) SEM-EDX analysis of the GDE's surface

The Bi_2O_3 catalyst show a very high activity as was expected based on literature.[31] In a comparing experiment where both a new In_2O_3 GDE as well as a new Bi_2O_3 GDE was used, the Bi_2O_3 showed a consistent higher faradaic efficiency with a significantly lower needed potential than In_2O_3 (Figure 9). Surprisingly though, the Bi-In (50:50)

catalyst shows a much lower efficiency below 60%. The striking difference with available literature[32] raises the interest to study different metal ratios to see if we can still achieve higher faradaic efficiencies with this bimetallic catalyst.

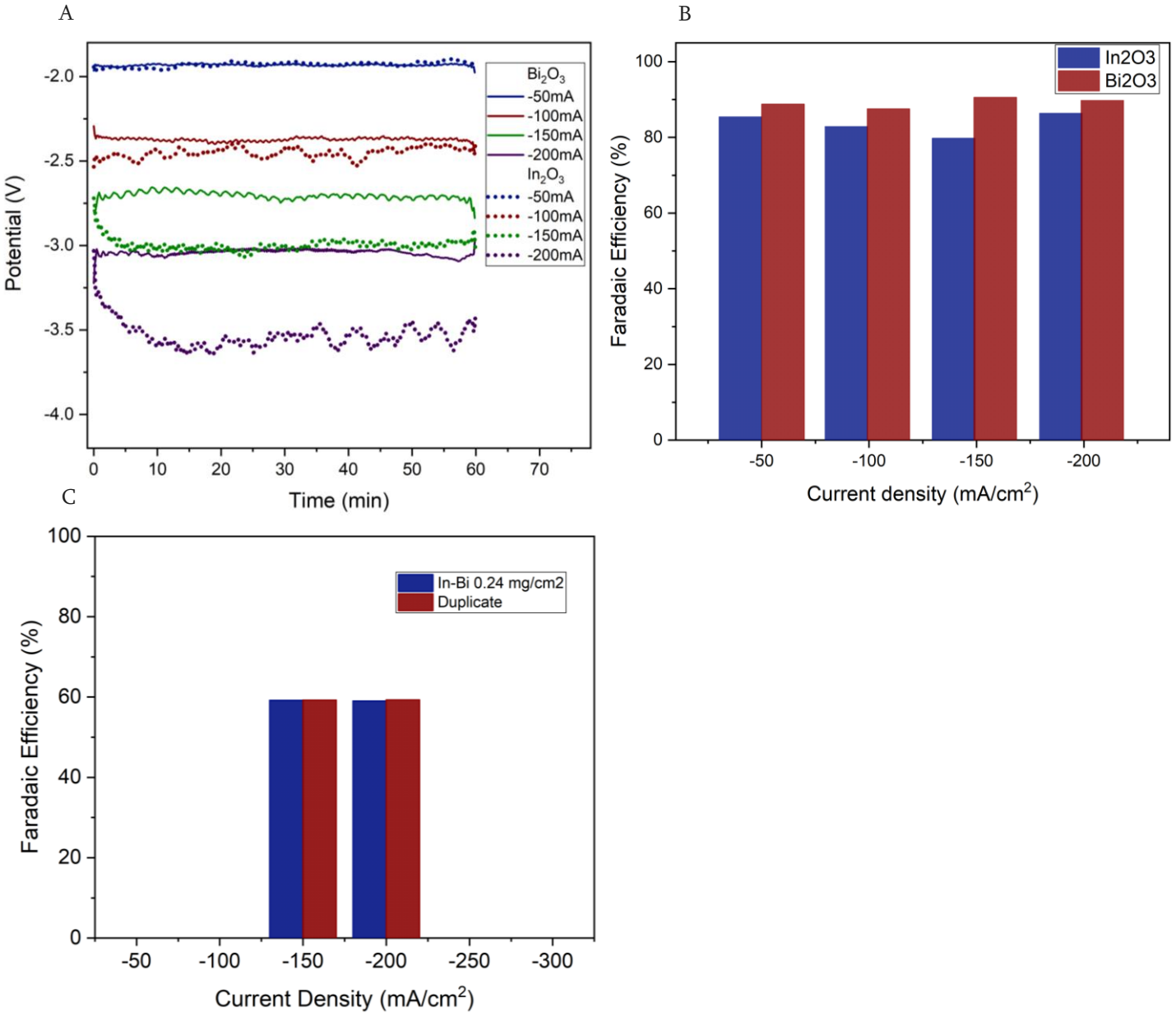

Figure 9: Comparison of In2O3, Bi2O3 and In-Bi oxide catalysts in CO2 reduction to formate at ambient conditions, a) recorded potentials for CP at 50 to 200 mA/cm2, b) corresponding FE of In2O3 and Bi2O3, c) FE on In-Bi oxide.

These Bi_2O_3 and In_2O_3 have been subjected to a stability tests of 9 hours (Figure 10). Despite some problems with some of the periodical concentration measurements, it is observed that after 9 hours the FE can be maintained at 50%. The figure below does show a very constant potential over time to reach 150 mA/cm^2, giving a first

indication of the stability of these catalyst for the first 9 hours. Further investigation on the stability of the catalyst will be extended to longer times and include post reaction analysis of the catalyst.

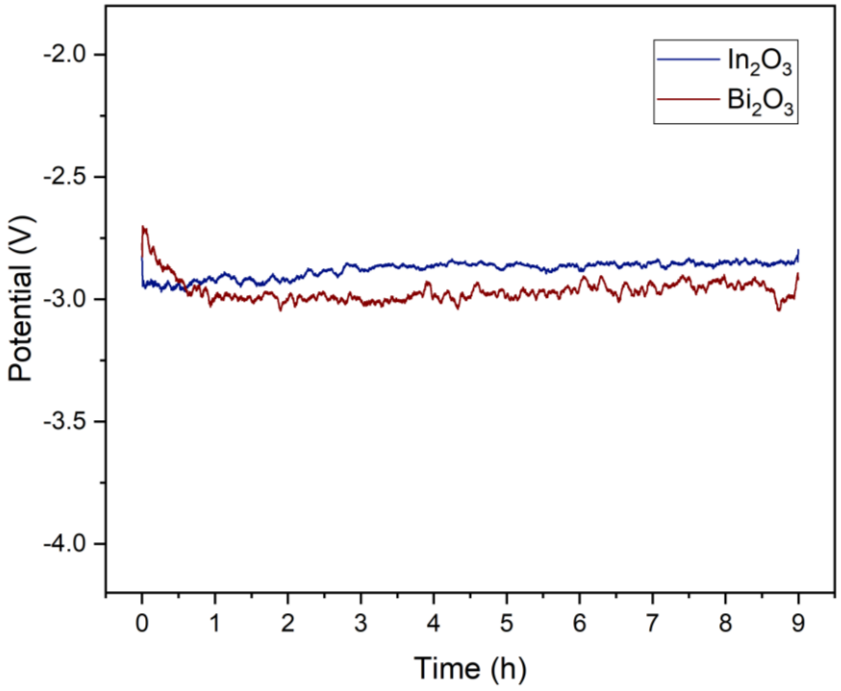

Figure 10: Stability tests on In_2O_3 and Bi_2O_3 GDE for 9h at ambient temperature and atmospheric pressure.

3 Conclusions and perspectives

For the hydrogenation of CO_2 to formic acid, Au commercial catalysts are chosen to proceed the studies. It was found in literature that activity and performance of this catalysts is high and not limiting the production. Moreover, it is a commercially available catalyst what brings further advantages concerning the applicability of the process at industrial scales. In the coming months, the efforts will be directed towards the modelling of the formic acid production (**Deliverable 4.5**).

For the electrochemical conversion, it was shown that the use of metal oxide nanoparticles made by flame spray pyrolysis for CO_2 reduction to formate shows excellent efficiencies at industrially relevant current densities. Doping In_2O_3 with Co, Cu, Pd, CeO_2 or ZrO_2 did not lead to increased efficiencies, but extended testing needs to verify these results. Pure Bi_2O_3 as well as In_2O_3 show very high efficiencies towards formate up to 90% with Bi_2O_3 performing slightly better and at lower overpotential. Surprisingly, the combination of Bi and In decreases the faradaic efficiency. Other metal ratios will be tested to increase the FE, aiming to achieve a 100%. Based on the results, the catalysts In_2O_3 and Bi_2O_3 will be prioritized for further investigation. We aim to investigate the influence of the morphology and composition during and after electrochemical CO_2 reduction as well as catalyst loading into the gas diffusion layer. Moreover, we will also investigate effects such as electrolyte pH, and electrolyte and gas flow rate on the selectivity and Faradaic efficiency. This will allow us to optimize the performance and stability of the catalyst and the reaction conditions for **Deliverable 4.4**.

4 References

1. Álvarez, A. *et al.* Challenges in the Greener Production of Formates/Formic Acid, Methanol, and DME by Heterogeneously Catalyzed CO2 Hydrogenation Processes. *Chem. Rev.* **117**, 9804–9838 (2017).
2. Hietala, J. *et al.* Formic Acid. in *Ullmann's Encyclopedia of Industrial Chemistry* **1**, 1–22 (Wiley-VCH Verlag GmbH & Co. KGaA, 2016).
3. Putten, R. Van, Wissink, T., Swinkels, T. & Pidko, E. A. ScienceDirect Fuelling the hydrogen economy : Scale-up of an integrated formic acid-to-power system. *Int. J. Hydrogen Energy* 1–9 (2019). doi:10.1016/j.ijhydene.2019.01.153
4. Bulushev, D. A. & Ross, J. R. H. Heterogeneous catalysts for hydrogenation of CO2 and bicarbonates to formic acid and formates. *Catal. Rev. - Sci. Eng.* **60**, 566–593 (2018).
5. Gunasekar, G. H., Park, K., Jung, K. D. & Yoon, S. Recent developments in the catalytic hydrogenation of CO2 to formic acid/formate using heterogeneous catalysts. *Inorg. Chem. Front.* **3**, 882–895 (2016).
6. Preti, D., Resta, C., Squarcialupi, S. & Fachinetti, G. Carbon dioxide hydrogenation to formic acid by using a heterogeneous gold catalyst. *Angew. Chemie - Int. Ed.* **50**, 12551–12554 (2011).
7. Filonenko, G. A., Vrijburg, W. L., Hensen, E. J. M. & Pidko, E. A. On the activity of supported Au catalysts in the liquid phase hydrogenation of CO2 to formates. *J. Catal.* **343**, 97–105 (2016).
8. Preti, D., Squarcialupi, S. & Fachinetti, G. Production of HCOOH/NEt3 Adducts by CO2/H2 Incorporation into Neat NEt3. *Angew. Chemie - Int. Ed.* **49**, 2581–2584 (2010).
9. Preti, D., Squarcialupi, S. & Fachinetti, G. Conversion of Syngas into Formic Acid. *ChemCatChem* **4**, 469–471 (2012).
10. Fachinetti, G. & Preti, D. PROCESS FOR PREPARING FORMIC ACID. (2012).
11. Schaub, T. & Paciello, R. A. A process for the synthesis of formic acid by CO2 hydrogenation: Thermodynamic aspects and the role of CO. *Angew. Chemie - Int. Ed.* **50**, 7278–7282 (2011).
12. Du, D., Lan, R., Humphreys, J. & Tao, S. Progress in inorganic cathode catalysts for electrochemical conversion of carbon dioxide into formate or formic acid. *J. Appl. Electrochem.* **47**, 661–678 (2017).
13. Ramdin, M. *et al.* High Pressure Electrochemical Reduction of CO2 to Formic Acid/Formate: A Comparison between Bipolar Membranes and Cation Exchange Membranes. *Ind. Eng. Chem. Res.* **58**, 1834–1847 (2019).
14. Ding, P. *et al.* Metal-based electrocatalytic conversion of CO2 to formic acid/formate. *J. Mater. Chem. A* (2020). doi:10.1039/d0ta08393c
15. Feaster, J. T. *et al.* Understanding Selectivity for the Electrochemical Reduction of Carbon Dioxide to Formic Acid and Carbon Monoxide on Metal Electrodes. *ACS Catal.* **7**, 4822–4827 (2017).
16. Liu, G., Tran-Phu, T., Chen, H. & Tricoli, A. A Review of Metal- and Metal-Oxide-Based Heterogeneous Catalysts for Electroreduction of Carbon Dioxide. *Adv. Sustain. Syst.* **2**, 1–13 (2018).
17. Hori, Y. Electrochemical CO2 Reduction on Metal Electrodes. in *Modern Aspects of Electrochemistry* (eds. Vayenas, C. G., White, R. E. & Gamboa-Aldeco, M. E.) **42**, (Springer New York, 2008).
18. Burdyny, T. & Smith, W. A. CO2 reduction on gas-diffusion electrodes and why catalytic performance must be assessed at commercially-relevant conditions. *Energy Environ. Sci.* **12**, 1442–1453 (2019).
19. Hori, Y. CO2 Reduction Using Electrochemical Approach. in *Solar to Chemical Energy Conversion* (eds. Sugiyama, M., Fujii, K. & Nakamura, S.) **32**, 191–211 (Springer International Publishing, 2016).
20. Teoh, W. Y., Amal, R. & Mädler, L. Flame spray pyrolysis: An enabling technology for nanoparticles design and fabrication. *Nanoscale* **2**, 1324–1347 (2010).
21. Gao, S. *et al.* Partially oxidized atomic cobalt layers for carbon dioxide electroreduction to liquid fuel. *Nature* **529**, 68–71 (2016).
22. Kortlever, R., Balemans, C., Kwon, Y. & Koper, M. T. M. Electrochemical CO2 reduction to formic acid

on a Pd-based formic acid oxidation catalyst. *Catal. Today* **244**, 58–62 (2015).
23. Min, X. & Kanan, M. W. Pd-Catalyzed Electrohydrogenation of Carbon Dioxide to Formate: High Mass Activity at Low Overpotential and Identification of the Deactivation Pathway. *J. Am. Chem. Soc.* **137**, 4701–4708 (2015).
24. Lu, X., Wu, Y., Yuan, X. & Wang, H. An Integrated CO 2 Electrolyzer and Formate Fuel Cell Enabled by a Reversibly Restructuring Pb–Pd Bimetallic Catalyst. *Angew. Chemie - Int. Ed.* **58**, 4031–4035 (2019).
25. Pereira-Hernández, X. I. *et al.* Tuning Pt-CeO 2 interactions by high-temperature vapor-phase synthesis for improved reducibility of lattice oxygen. *Nat. Commun.* **10**, (2019).
26. Dutta, A., Kuzume, A., Rahaman, M., Vesztergom, S. & Broekmann, P. Monitoring the Chemical State of Catalysts for CO2 Electroreduction: An In Operando Study. *ACS Catal.* **5**, 7498–7502 (2015).
27. Reske, R., Mistry, H., Behafarid, F., Roldan Cuenya, B. & Strasser, P. Particle size effects in the catalytic electroreduction of CO2 on Cu nanoparticles. *J. Am. Chem. Soc.* **136**, 6978–6986 (2014).
28. Vennekoetter, J.-B., Sengpiel, R. & Wessling, M. Beyond the catalyst: How electrode and reactor design determine the product spectrum during electrochemical CO2 reduction. *Chem. Eng. J.* **364**, 89–101 (2019).
29. García de Arquer, F. P. *et al.* CO2 electrolysis to multicarbon products at activities greater than 1 A cm–2. *Science (80-.).* **367**, 661–666 (2020).
30. Yoo, J. S., Christensen, R., Vegge, T., Nørskov, J. K. & Studt, F. Theoretical Insight into the Trends that Guide the Electrochemical Reduction of Carbon Dioxide to Formic Acid. *ChemSusChem* **9**, 358–363 (2016).
31. Fan, L., Xia, C., Zhu, P., Lu, Y. & Wang, H. Electrochemical CO2 reduction to high-concentration pure formic acid solutions in an all-solid-state reactor. *Nat. Commun.* **11**, 1–9 (2020).
32. Kaczur, J. J., Lakkaraju, P. & Teamey, K. Method and System for Electrochemical Reduction of Carbon Dioxide employing a Gas Diffusion Anode. (2019).